Physical Communication 35 (2019) 100729

Contents lists available at ScienceDirect

Physical Communication

journal homepage: www.elsevier.com/locate/phycom

Full length article

Performance of a relay-assisted hybrid FSO/RF communication system

Mohammad Ali Amirabadi *, Vahid Tabataba Vakili

School of Electrical Engineering, Iran University of Science and Technology (IUST), Tehran 1684613114, Iran

ARTICLE INFO

Article history:
Received 17 September 2018
Received in revised form 1 June 2019
Accepted 4 June 2019
Available online 12 June 2019

Keywords:
Free space optic/radio frequency
Gamma–Gamma
Negative exponential
Pointing error
Relay-assisted
Multi-user

ABSTRACT

This paper investigates the performance of a multi-user relay-assisted hybrid Free Space Optical/Radio Frequency (FSO/RF) communication system. The proposed dual-hop structure is particularly suitable for areas, in which direct RF communication between mobile users and base station is not possible due to bad channel conditions. In this system, mobile users are connected to the base station with the help of a fixed gain or adaptive gain amplify and forward relay. It is the first time that effect of the number of users on the performance of a dual-hop hybrid FSO/RF structure is investigated. Also, it is the first time that the performance of a dual-hop hybrid FSO/RF is investigated in Negative Exponential atmospheric turbulence (saturate atmospheric turbulence regime). Considering FSO link at a wide range of atmospheric turbulence regimes, from moderate to saturate, closed-form expressions are derived for Bit Error Rate (BER) and outage probability (P_{out}) of the proposed structure. The MATLAB simulations verified the accuracy of the derived expressions. It is shown that the performance of adaptive gain relaying is less sensitive to the number of users; therefore, this structure is suitable for areas with variable population density. Fixed gain relaying is shown to perform better than adaptive gain relaying. This is because although the fixed gain scheme has low complexity, it assumes much more power, which causes favorable even in the worst case scenario. Therefore, this structure is suitable for the situation that the relay could not deserve much complexity. Accordingly and due to favorable performance at a wide range of atmospheric turbulence, the proposed structure is a special case for low cost, low complexity, and reliable communication.

1. Introduction

Free Space Optical (FSO) communication system is a timely field of research study [1,2]. This is due to the high data rate, bandwidth, security, unlicensed spectrum, as well as easy and low-cost installation [3,4]. In contrast to these advantages, the FSO system is highly sensitive to atmospheric turbulence, and the effect of pointing error. Scintillation, as an effect of atmospheric turbulence, fluctuates the intensity of the received light and degrades the performance of FSO system [5,6]. This effect could be reduced by aperture averaging technique, in which the receiver aperture diameter is changed adaptively based on Channel State Information (CSI). The pointing error effect, which is caused by building sway in the wind, small earthquakes, and building vibrations, severely affects the performance of FSO system [7–10]. However, it could be reduced by increasing the beam diameter [11]. In order to investigate the effects of atmospheric turbulence and pointing error on the performance of FSO system, various statistical distributions have been released. The lognormal distribution is used to model weak atmospheric turbulence [12], Gamma–Gamma distribution is used to model weak to strong atmospheric turbulence [13–16], and Negative Exponential distribution is used to model saturate atmospheric turbulence [17].

Impacts of communication channel on FSO and millimeter wave Radio Frequency (RF) signals are not the same; for example, in FSO link the main performance degradation factors are pointing error and atmospheric turbulence, and the rain does not affect it so much; in contrast, RF link is sensitive to heavy rain and does not care about pointing error and atmospheric turbulence [18]. Actually, FSO and RF links are the complements of each other, and their combination increases link reliability and improves system performance [19]. The so-called hybrid FSO/RF systems are available in parallel and series structures. In parallel structure, either both FSO and RF links transmit data at the same time or one of them transmit data and the other one acts as a back-up link. In series structures, FSO and RF links are connected through a relay station [11]. These systems have advantages of FSO, RF, and relay-assisted systems, such as high bandwidth, reliability, accessibility, and performance. Actually, in areas with bad channel conditions, mobile users might not be able to communicate with the base station, therefore, the series structure could be really useful in these areas.

* Corresponding author.
E-mail addresses: m_amirabadi@elec.iust.ac.ir (M.A. Amirabadi), Vakili@iust.ac.ir (V. Tabataba Vakili).

https://doi.org/10.1016/j.phycom.2019.100729
1874-4907/

Different relaying protocols have been used in relay-assisted hybrid FSO/RF system, for example, amplify and forward, decode and forward, demodulate and forward; among them amplify and forward is very simple and mostly used [11]. Because it does not need any demodulating or decoding or detecting at the relay, it just amplifies the received signal with fixed or adaptive gain (based on the availability of CSI at the relay) and forwards it. Therefore, this protocol is suitable for the long-range link, bad communication channel conditions, or situations with power demand on the transmitter side. According that this paper tries to investigate performance at saturate regime of atmospheric turbulence, amplify and forward is selected as relay protocol. In addition, the considered link (between mobile and base station) is short and using amplify and forward (lonely) results in favorable performance (see results); so, there is no need to decode before amplification. The fixed gain scheme has low complexity, and is flexible because the amplification gain could be selected manually; by selecting a high amplification gain (and correspondingly assuming more power), it could have favorable performance even at worst case scenario. On the other hand, the adaptive gain scheme has more complexity (requires CSI) and its gain is changed based on channel CSI.

Various Direct Detection/Intensity Modulation (IM /DD) formats are used in the FSO systems. One of the most widely used modulations is On–Off keying (OOK), in which detection must be done according to a threshold based on CSI. Another well-known modulation is pulse position modulation (PPM) that does not require adaptive threshold detection but has less spectral efficiency than OOK. Subcarrier intensity modulation (SIM), due to higher spectral efficiency over PPM and OOK, is an appropriate alternative for PPM and OOK but requires carrier phase and frequency synchronization [20].

The current dual-hop hybrid FSO/RF links could be divided into two main categories, including with [21–25] and without [11,26–39] direct (back-up) connection between source and destination; each of these two categories could be divided into two main subcategories, including single-user [11,23,24,27,30–32,36–40] and multi-user [21,22,26,28,29,33–35]. In multi-user schemes, different allocation approaches are used. The Gamma–Gamma atmospheric turbulence, (due to high accompany with experimental results for weak to strong regime) is mostly used in FSO link [11,21–24,26–31,34,36–40]; however, some works considered M-distribution [32,33,41,42], Exponential Weibull [35], and Alpha-Mu [25] distributions. Again, due to high accompany with experimental results, (in Line Of Sight links) the Rayleigh fading [21,23,27,31–33,36–39] and (in multi-path links) the Nakagami-m [11,22,28–30,34–36] fading are mostly considered for RF link, and few works considered Rician distribution [26].

According to the above literature review, and to the best of authors' knowledge, the novelties and contributions of this system (among dual-hop hybrid FSO/RF systems) include: considering the selection of the best user scenario (in multi-user system), considering wide range of atmospheric turbulence from moderate to saturate, considering Negative exponential distribution (saturate atmospheric turbulence regime), investigating the effect of number of users on the performance. In this paper, a multi-user relay-assisted hybrid FSO/RF communication system is presented. In this structure, mobile users are connected to the base station with the help of either fixed gain or adaptive gain amplify and forward relay. The first link is RF with Rayleigh fading, the second link is FSO with Gamma–Gamma atmospheric turbulence considering the effect of pointing error (in moderate to strong regimes), and Negative Exponential atmospheric turbulence (in saturate regime). Closed form expressions are derived for BER and P_{out} of the proposed system, and verified through MATLAB simulations. According to characteristics of FSO, RF, and the relay-assisted system it is expected that the proposed structure shows reliable communication at a wide range of atmospheric turbulence and population density.

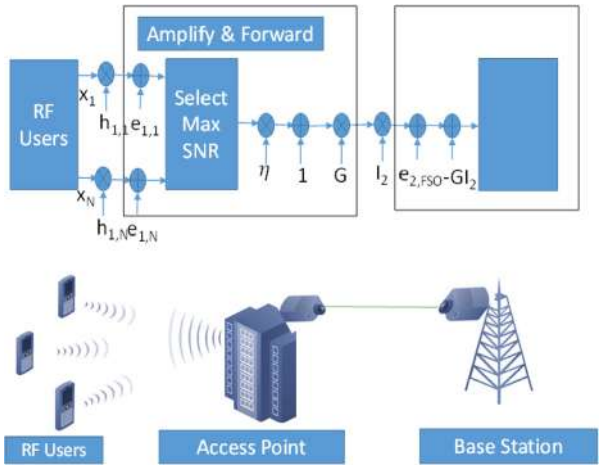

Fig. 1. Proposed relay-assisted hybrid FSO/RF system.

Rest of the paper is organized as follows: In Section 2, the proposed relay assisted hybrid FSO/RF system model is presented. Section 3 studies the performance of the fixed gain scheme and Section 4 studies performance of the adaptive gain scheme. Section 5 dedicates to the comparison of analytic and simulation results, and Section 6 is the conclusion of this paper.

2. System model

Fig. 1 depicts the proposed dual-hop relay-assisted hybrid FSO/RF system. In this structure, mobile users are connected to the relay via RF link; the relay is connected to the base station via FSO link. Among received RF signals, one with the highest Signal to Noise Ratio (SNR) is selected and then converted to FSO signal with the conversion efficiency of η; a DC bias with unit amplitude is added to the FSO signal in order to be positive. This signal is amplified and forwarded through FSO link, and finally detected at the base station.

Considering $x_i; i = 1, 2, \ldots, N$ as the transmitted RF signal from ith mobile user, the received signal at the relay becomes as follows:

$$y_{RF,i} = h_i x_i + e_{RF,i}, \tag{1}$$

where h_i (the fading coefficient of ith RF path) is complex Gaussian random variable [17]; $e_{RF,i}$ (relay input noise) is Additive White Gaussian Noise (AWGN) with zero mean and σ^2_{RF} variance. At the relay, received signal with the highest SNR is selected in the following form:

$$\gamma_{RF} = max(\gamma_{RF,1}, \gamma_{RF,2}, \ldots, \gamma_{RF,N}). \tag{2}$$

Received RF signal at the relay is first converted to an electrical signal (this issue is done by the resonation part of the relay; resonator converts RF signal to electrical signal but does not change the frequency); the frequency range of this signal is on the order of RF frequency. With the help of optical modulators (Mach Zehnder Modulator should be used, because the RF signal has Differential Phase Shift Keying (DPSK) modulation, which should be retained in FSO signal) the electrical signal is then got on an optical carrier (the frequency of the produced FSO signal is on the order of optical signals). After conversion from RF signal to FSO signal, relay adds a unit amplitude DC bias, then amplifies and forwards it to the base station as follows:

$$x_R = G\,(1 + \eta y_{RF})\,, \tag{3}$$

where G is the amplification gain and y_{RF} is selected RF signal. After DC removal, received FSO signal at the base station becomes as follows:

$$y_{FSO} = I_2 x_R + e_{FSO} - I_2 G = I_2 G\eta\,(hx_i + e_{RF}) + e_{FSO}, \tag{4}$$

where I_2 is atmospheric turbulence intensity and e_{FSO} (the base station input noise) is AWGN with σ^2_{FSO} variance and zero mean. Instantaneous SNR at base station becomes as [32]:

$$\gamma_{FSO/RF} = \frac{I_2^2 G^2 \eta^2 h^2}{I_2^2 G^2 \eta^2 \sigma_{RF}^2 + \sigma_{FSO}^2} = \frac{\frac{I_2^2\eta^2}{\sigma_{FSO}^2}\frac{h^2}{\sigma_{RF}^2}}{\frac{I_2^2\eta^2}{\sigma_{FSO}^2} + \frac{1}{G^2\sigma_{RF}^2}}, \tag{5}$$

where the signal power is assumed to be unit ($E\left[x_i^2\right] = 1$). In the case of un-known CSI, the received signal is amplified with fixed gain ($G^2 = 1/(C\sigma_{RF}^2)$) [32], where C is a desired constant parameter. By substitution of G, $\gamma_{RF} = h^2/\sigma_{RF}^2$, and $\gamma_{FSO} = \eta^2 I_2^2/\sigma_{FSO}^2$ in (5), instantaneous SNR at base station input for fixed gain scheme becomes as:

$$\gamma_{FSO/RF} = \frac{\gamma_{FSO}\gamma_{RF}}{\gamma_{FSO} + C}. \tag{6}$$

If γ_{RF} and γ_{FSO} tend to infinity, then $\gamma_{FSO/RF} \cong \gamma_{RF}$. Therefore, in fixed gain relaying, at high SNRs, the proposed structure performs independently at different atmospheric turbulence regimes. When CSI is known, received signal at the relay would be amplified with adaptive gain ($G^2 = 1/(h^2+\sigma_{RF}^2)$) [32]. Adaptive gain relaying needs channel estimation but fixed gain scheme does not. Substituting G, $\gamma_{RF} = h^2/\sigma_{RF}^2$, and $\gamma_{FSO} = \eta^2 I_2^2/\sigma_{FSO}^2$ in (5), instantaneous SNR at base station input for adaptive gain scheme becomes:

$$\gamma_{FSO/RF} = \frac{\gamma_{FSO}\gamma_{RF}}{\gamma_{FSO} + \gamma_{RF} + 1}. \tag{7}$$

If γ_{RF} and γ_{FSO} tend to infinity, then $\gamma_{FSO/RF} \cong \min(\gamma_{FSO}, \gamma_{RF})$. Therefore, in adaptive gain relaying, at high SNRs, the proposed structure performs independent of link with lower SNR.

Probability density function (pdf) of Gamma–Gamma distribution with the effect of pointing errors is as [29]:

$$f_{\gamma_{FSO}}(\gamma) = \frac{\xi^2}{2\Gamma(\alpha)\Gamma(\beta)\gamma} G_{1,3}^{3,0}\left(\alpha\beta\kappa\sqrt{\frac{\gamma}{\overline{\gamma}_{FSO}}}\,\middle|\,\begin{matrix}\xi^2+1\\ \xi^2, \alpha, \beta\end{matrix}\right), \tag{8}$$

where $G_{p,q}^{m,n}\left(z\,\middle|\,\begin{matrix}a_1, a_2, \ldots, a_p\\ b_1, b_2, \ldots, b_q\end{matrix}\right)$ is Meijer-G function, α, β are parameters related to Gamma–Gamma atmospheric turbulence intensity, ξ^2 is related to the effect of pointing errors and $\Gamma(.)$ is Gamma function [43]. $\xi^2 = \omega_{Z_{eq}}/(2\sigma_s)$ is ratio between equivalent beam diameter and pointing error displacement standard deviation (jitter) at the receiver. Where σ_s^2 is the jitter variance and $\omega_{Z_{eq}}$ is equivalent beam radius at the receiver. α, β are defined as $\alpha = \left[\exp\left(0.49\sigma_R^2/(1+1.11\sigma_R^{\frac{12}{5}})^{\frac{7}{6}}\right) - 1\right]^{-1}$ and $\beta = \left[\exp\left(0.51\sigma_R^2/(1+0.69\sigma_R^{\frac{12}{5}})^{\frac{5}{6}}\right) - 1\right]^{-1}$, where σ_R^2 is the Rytov variance [29]. Average SNR at the FSO receiver input is $\overline{\gamma}_{FSO} = 1/\sigma_{FSO}^2$.

Cumulative Distribution Function (CDF) of Gamma–Gamma distribution with the effect of pointing error is as follows [29]:

$$F_{\gamma_{FSO}}(\gamma) = \frac{\xi^2}{\Gamma(\alpha)\Gamma(\beta)} G_{2,4}^{3,1}\left(\alpha\beta\kappa\sqrt{\frac{\gamma}{\overline{\gamma}_{FSO}}}\,\middle|\,\begin{matrix}1, \xi^2+1\\ \xi^2, \alpha, \beta, 0\end{matrix}\right). \tag{9}$$

The pdf and CDF of Negative Exponential distribution with $1/\lambda^2$ variance and $1/\lambda$ mean are respectively as follows:

$$f_{\gamma_{FSO}}(\gamma) = \frac{\lambda}{2\sqrt{\gamma\overline{\gamma}_{FSO}}} e^{-\lambda\sqrt{\frac{\gamma}{\overline{\gamma}_{FSO}}}}. \tag{10}$$

$$F_{\gamma_{FSO}}(\gamma) = 1 - e^{-\lambda\sqrt{\frac{\gamma}{\overline{\gamma}_{FSO}}}}. \tag{11}$$

Fading distribution of ith RF path is Rayleigh and its variance is assumed to be the same in all paths ($\overline{\gamma}_{RF,i} = \overline{\gamma}_{RF}$). The pdf of $\gamma_{RF,i}$ random variable is as follows [32]:

$$f_{\gamma_{RF,i}}(\gamma) = \frac{1}{\overline{\gamma}_{RF}} e^{-\frac{\gamma}{\overline{\gamma}_{RF}}}. \tag{12}$$

Integrating the above equation, CDF of $\gamma_{RF,i}$ random variable becomes as follows:

$$F_{\gamma_{RF,i}}(\gamma) = 1 - e^{-\frac{\gamma}{\overline{\gamma}_{RF}}}. \tag{13}$$

Using (2), CDF of the entire RF link is as follows:

$$\begin{aligned} F_{\gamma_{RF}}(\gamma) &= Pr\left(\max\left(\gamma_{RF,1}, \gamma_{RF,2}, \ldots, \gamma_{RF,N}\right) \le \gamma\right) \\ &= Pr\left(\gamma_{RF,1} \le \gamma, \gamma_{RF,2} \le \gamma, \ldots, \gamma_{RF,N} \le \gamma\right). \end{aligned} \tag{14}$$

Assuming independence for RF paths, CDF of the entire RF link becomes as follows:

$$F_{\gamma_{RF}}(\gamma) = \prod_{i=1}^{N} Pr\left(\gamma_{RF,i} \le \gamma\right) = \prod_{i=1}^{N} F_{\gamma_{RF,i}}(\gamma). \tag{15}$$

Assuming identical distribution for RF paths, CDF of entire RF link becomes as follows:

$$F_{\gamma_{RF}}(\gamma) = \left(F_{\gamma_{RF,i}}(\gamma)\right)^N = \left(1 - e^{-\frac{\gamma}{\overline{\gamma}_{RF}}}\right)^N. \tag{16}$$

By derivation of (16), pdf of entire RF link becomes as follows:

$$\begin{aligned} f_{\gamma_{RF}}(\gamma) &= N\left(F_{\gamma_{RF,i}}(\gamma)\right)^{N-1} f_{\gamma_{RF,i}}(\gamma) \\ &= \frac{N}{\overline{\gamma}_{RF}} e^{-\frac{\gamma}{\overline{\gamma}_{RF}}}\left(1 - e^{-\frac{\gamma}{\overline{\gamma}_{RF}}}\right)^{N-1}. \end{aligned} \tag{17}$$

Substituting binomial expansion of $\left(1 - e^{-\gamma/\overline{\gamma}_{RF}}\right)^{N-1}$ as $\sum_{k=0}^{N-1}\binom{N-1}{k}(-1)^k e^{-k\gamma/\overline{\gamma}_{RF}}$ in (17), pdf of entire RF link becomes as follows:

$$f_{\gamma_{RF}}(\gamma) = \frac{N}{\overline{\gamma}_{RF}} \sum_{k=0}^{N-1}\binom{N-1}{k}(-1)^k e^{-\frac{(k+1)\gamma}{\overline{\gamma}_{RF}}}. \tag{18}$$

3. Performance of fixed gain structure

3.1. Outage probability

The outage occurs when instantaneous SNR comes down below a threshold level (γ_{th}). According to this definition, P_{out} of the proposed system can be written as follows:

$$\begin{aligned} P_{out,\gamma_{FSO/RF}}(\gamma_{th}) &= Pr\left(\gamma_{FSO/RF} \le \gamma_{th}\right) = 1 - Pr\left(\gamma_{\frac{FSO}{RF}} \ge \gamma_{th}\right) \\ &= 1 - Pr\left(\frac{\gamma_{FSO}\gamma_{RF}}{\gamma_{FSO} + C} \ge \gamma_{th}\right). \end{aligned} \tag{19}$$

After mathematical simplification, (19) becomes as follows [27]:

$$= 1 - \int_0^\infty Pr\left(\gamma_{FSO} \ge \frac{\gamma_{th} C}{x} | \gamma_{RF}\right) f_{\gamma_{RF}}(x + \gamma_{th})\, dx. \tag{20}$$

Substituting (9) and (18) into (20) and after mathematical simplification, P_{out} of the proposed system in Gamma–Gamma atmospheric turbulence considering pointing error becomes as follows:

$$P_{out,\gamma_{FSO/RF}}(\gamma_{th}) = 1 - \frac{N}{\overline{\gamma}_{RF}} \sum_{k=0}^{N-1} \binom{N-1}{k} (-1)^k e^{-\frac{(k+1)\gamma_{th}}{\overline{\gamma}_{RF}}} \times \left[\int_0^\infty e^{-\frac{(k+1)x}{\overline{\gamma}_{RF}}} dx - \frac{\xi^2}{\Gamma(\alpha)\Gamma(\beta)} \int_0^\infty e^{-\frac{(k+1)x}{\overline{\gamma}_{RF}}} G_{2,4}^{3,1} \times \left(\alpha\beta\kappa \sqrt{\frac{\gamma_{th}C}{x\overline{\gamma}_{FSO}}} \middle| \begin{matrix} 1, \xi^2+1 \\ \xi^2, \alpha, \beta, 0 \end{matrix} \right) dx \right]. \quad (21)$$

Substituting equivalent of $G_{2,4}^{3,1}\left(\alpha\beta\kappa\sqrt{\frac{\gamma_{th}C}{x\overline{\gamma}_{FSO}}}\middle|\begin{matrix}1,\xi^2+1\\ \xi^2,\alpha,\beta,0\end{matrix}\right)$ as $G_{4,2}^{1,3}\left(\frac{1}{\alpha\beta\kappa}\sqrt{\frac{x\overline{\gamma}_{FSO}}{\gamma_{th}C}}\middle|\begin{matrix}1-\xi^2,1-\alpha,1-\beta,1\\ 0,-\xi^2\end{matrix}\right)$ [44, Eq. 07.34.17.0012.01] and by using [44, Eq. 07.34.21.0088.01], P_{out} of the proposed system in Gamma–Gamma atmospheric turbulence with the effect of pointing errors becomes as follows:

$$P_{out,\gamma_{FSO/RF}}(\gamma_{th}) = 1 - \sum_{k=0}^{N-1} \binom{N-1}{k} (-1)^k \frac{N}{k+1} e^{-\frac{(k+1)\gamma_{th}}{\overline{\gamma}_{RF}}} \times \left[1 - \frac{\xi^2 2^{\alpha+\beta-3}}{\pi\Gamma(\alpha)\Gamma(\beta)} \times G_{9,4}^{2,7} \times \left(\frac{16\overline{\gamma}_{FSO}\overline{\gamma}_{RF}}{(\alpha\beta\kappa)^2 \gamma_{th}C(k+1)} \middle| \begin{matrix} 0, \frac{1-\xi^2}{2}, \frac{2-\xi^2}{2}, \frac{1-\alpha}{2}, \frac{2-\alpha}{2}, \frac{1-\beta}{2}, \frac{2-\beta}{2}, \frac{1}{2}, 1 \\ 0, \frac{1}{2}, -\frac{\xi^2}{2}, \frac{1-\xi^2}{2} \end{matrix} \right) \right]. \quad (22)$$

Substituting (11) and (18) into (20), and after mathematical simplification, P_{out} of the proposed system in Negative Exponential atmospheric turbulence becomes as follows:

$$P_{out,\gamma_{FSO/RF}}(\gamma_{th}) = 1 - \frac{N}{\overline{\gamma}_{RF}} \sum_{k=0}^{N-1} \binom{N-1}{k} (-1)^k e^{-\frac{(k+1)\gamma_{th}}{\overline{\gamma}_{RF}}} \times \int_0^\infty e^{-\frac{(k+1)x}{\overline{\gamma}_{RF}}} e^{-\lambda\sqrt{\frac{\gamma_{th}C}{x\overline{\gamma}_{FSO}}}} dx. \quad (23)$$

From [44, Eq. 07.34.17.0012.01] and [44, Eq. 07.34.03.1081.01] Meijer-G equivalent of $e^{-\lambda\sqrt{C\gamma_{th}/(x\overline{\gamma}_{FSO})}}$ is equal to $\frac{1}{\sqrt{\pi}} G_{2,0}^{0,2}\left(4x\overline{\gamma}_{FSO}\lambda^2 \gamma_{th}C \middle| \begin{matrix} 1, 1/2 \\ - \end{matrix}\right)$. Substituting it and using [44, Eq. 07.34.21.0088.01] P_{out} of the proposed system in Negative Exponential atmospheric turbulence becomes as follows:

$$P_{out,\gamma_{FSO/RF}}(\gamma_{th}) = 1 - \sum_{k=0}^{N-1} \binom{N-1}{k} (-1)^k \frac{N}{\sqrt{\pi}(k+1)} e^{\frac{(k+1)\gamma_{th}}{\overline{\gamma}_{RF}}} \times G_{3,0}^{0,3}\left(\frac{4\overline{\gamma}_{FSO}\overline{\gamma}_{RF}}{\lambda^2\gamma_{th}C(k+1)} \middle| \begin{matrix} \frac{0,1,1}{2} \\ - \end{matrix} \right). \quad (24)$$

3.2. Bit error rate

Although MPSK modulations have better BER performance than DPSK, the DPSK receiver does not require a carrier phase estimation circuit and has low complexity. Given that $F_\gamma(\gamma) = P_{out}(\gamma)$, BER of DPSK modulation can be obtained from the following equation [32,45]:

$$P_e = \frac{1}{2}\int_0^\infty e^{-\gamma} F_\gamma(\gamma)\, d\gamma = \frac{1}{2}\int_0^\infty e^{-\gamma} P_{out}(\gamma)\, d\gamma \quad (25)$$

Substituting (22) into (25), BER of DPSK modulation over Gamma–Gamma atmospheric turbulence considering pointing error is equal to:

$$= \frac{1}{2}\int_0^\infty e^{-\gamma} \left\{ 1 - \sum_{k=0}^{N-1} \binom{N-1}{k} (-1)^k \frac{N}{k+1} e^{\frac{(k+1)\gamma}{\overline{\gamma}_{RF}}} \times \left[1 - \frac{\xi^2 2^{\alpha+\beta-3}}{\pi\Gamma(\alpha)\Gamma(\beta)} \times G_{9,4}^{2,7} \times \left(\frac{16\overline{\gamma}_{FSO}\overline{\gamma}_{RF}}{(\alpha\beta\kappa)^2\gamma C(k+1)} \middle| \begin{matrix} 0, \frac{1-\xi^2}{2}, \frac{2-\xi^2}{2}, \frac{1-\alpha}{2}, \frac{2-\alpha}{2}, \frac{1-\beta}{2}, \frac{2-\beta}{2}, \frac{1}{2}, 1 \\ 0, \frac{1}{2}, \frac{-\xi^2}{2}, \frac{1-\xi^2}{2} \end{matrix} \right) \right] d\gamma \right\}. \quad (26)$$

Substituting equivalent of $G_{9,4}^{2,7}\left(\frac{16\overline{\gamma}_{FSO}\overline{\gamma}_{RF}}{(\alpha\beta\kappa)^2\gamma C(k+1)}\middle|\begin{matrix}0,\frac{1-\xi^2}{2},\frac{2-\xi^2}{2},\frac{1-\alpha}{2},\frac{2-\alpha}{2},\frac{1-\beta}{2},\frac{2-\beta}{2},\frac{1}{2},1\\ 0,\frac{1}{2},\frac{-\xi^2}{2},\frac{1-\xi^2}{2}\end{matrix}\right)$ as $G_{4,9}^{7,2}\left(\frac{(\alpha\beta\kappa)^2\gamma C(k+1)}{16\overline{\gamma}_{FSO}\overline{\gamma}_{RF}}\middle|\begin{matrix}1,\frac{1}{2},\frac{2+\xi^2}{2},\frac{1+\xi^2}{2}\\ 1,\frac{1+\xi^2}{2},\frac{\xi^2}{2},\frac{1+\alpha}{2},\frac{\alpha}{2},\frac{1+\beta}{2},\frac{\beta}{2},\frac{1}{2},0\end{matrix}\right)$ [44, Eq. 07.34.17.0012.01] and using [44, Eq. 07.34.21.0088.01] BER of DPSK modulation over Gamma–Gamma atmospheric turbulence with the effect of pointing error becomes equal to:

$$P_e = \frac{1}{2}\left\{ 1 - \sum_{k=0}^{N-1} \binom{N-1}{k} (-1)^k \frac{N}{k+1} \frac{1}{1+\frac{k+1}{\overline{\gamma}_{RF}}} \times \left[1 - \frac{\xi^2 2^{\alpha+\beta-3}}{\pi\Gamma(\alpha)\Gamma(\beta)} G_{5,9}^{7,3} \times \left(\frac{(\alpha\beta\kappa)^2 C(k+1)}{16\overline{\gamma}_{FSO}\left(\overline{\gamma}_{RF}+k+1\right)} \middle| \begin{matrix} 0, 1, \frac{1}{2}, \frac{2+\xi^2}{2}, \frac{1+\xi^2}{2} \\ 1, \frac{1+\xi^2}{2}, \frac{\xi^2}{2}, \frac{1+\alpha}{2}, \frac{\alpha}{2}, \frac{1+\beta}{2}, \frac{\beta}{2}, \frac{1}{2}, 0 \end{matrix} \right) \right] \right\}. \quad (27)$$

Substituting (24) into (25), BER of negative exponential atmospheric turbulence is equal to:

$$P_e = \frac{1}{2}\int_0^\infty e^{-\gamma} \left\{ 1 - \sum_{k=0}^{N-1} \binom{N-1}{k} (-1)^k \frac{N}{\sqrt{\pi}(k+1)} e^{\frac{(k+1)\gamma}{\overline{\gamma}_{RF}}} \times G_{3,0}^{0,3}\left(\frac{4\overline{\gamma}_{FSO}\overline{\gamma}_{RF}}{\lambda^2\gamma C(k+1)} \middle| \begin{matrix} 0, 1, \frac{1}{2} \\ - \end{matrix} \right) \right\} d\gamma. \quad (28)$$

Substituting equivalent of $G_{3,0}^{0,3}\left(\frac{4\overline{\gamma}_{FSO}\overline{\gamma}_{RF}}{\lambda^2\gamma C(k+1)}\middle|\begin{matrix}0,1,0.5\\ -\end{matrix}\right)$ as $G_{0,3}^{3,0}\left(\frac{\lambda^2\gamma C(k+1)}{4\overline{\gamma}_{FSO}\overline{\gamma}_{RF}}\middle|\begin{matrix}-\\ 1,0,0.5\end{matrix}\right)$ [44, Eq. 07.34.17.0012.01] and using [44, Eq. 07.34.21.0088.01], BER of Negative Exponential atmospheric turbulence is equal to:

$$P_e = \frac{1}{2}\left\{ 1 - \sum_{k=0}^{N-1} \binom{N-1}{k} (-1)^k \frac{N}{\sqrt{\pi}(k+1)} \frac{1}{1+\frac{k+1}{\overline{\gamma}_{RF}}} G_{1,3}^{3,1} \times \left(\frac{4\overline{\gamma}_{FSO}\overline{\gamma}_{RF}}{\lambda^2\gamma C(k+1)} \middle| \begin{matrix} 0 \\ 1, 0, \frac{1}{2} \end{matrix} \right) \right\}. \quad (29)$$

4. Performance of adaptive gain structure

4.1. Outage probability

(7) can be approximated as [32]:

$$\gamma_{FSO/RF} = \frac{\gamma_{FSO}\gamma_{RF}}{\gamma_{FSO}+\gamma_{RF}+1} \cong min(\gamma_{FSO}, \gamma_{RF}). \quad (30)$$

The CDF of $\gamma_{FSO/RF}$ random variable equals with [46]:

$$F_{\gamma_{FSO/RF}}(\gamma) = F_{\gamma_{RF}}(\gamma) + F_{\gamma_{FSO}}(\gamma) - F_{\gamma_{RF}}(\gamma) F_{\gamma_{FSO}}(\gamma). \quad (31)$$

Given that $P_{out}(\gamma_{th}) = F_{\gamma}(\gamma_{th})$, substituting (9) and (16) in (31), P_{out} of Gamma–Gamma atmospheric turbulence with the effect of pointing the error is equal to:

$$P_{out,\gamma_{FSO/RF}}(\gamma_{th}) = \left(1-e^{-\frac{\gamma_{th}}{\overline{\gamma}_{RF}}}\right)^N + \frac{\xi^2}{\Gamma(\alpha)\Gamma(\beta)} G_{2,4}^{3,1}\left(\alpha\beta\kappa\sqrt{\frac{\gamma_{th}}{\overline{\gamma}_{FSO}}}\,\middle|\,\begin{matrix}1,\xi^2+1\\ \xi^2,\alpha,\beta,0\end{matrix}\right) - \frac{\xi^2}{\Gamma(\alpha)\Gamma(\beta)}\left(1-e^{-\frac{\gamma_{th}}{\overline{\gamma}_{RF}}}\right)^N G_{2,4}^{3,1}\left(\alpha\beta\kappa\sqrt{\frac{\gamma_{th}}{\overline{\gamma}_{FSO}}}\,\middle|\,\begin{matrix}1,\xi^2+1\\ \xi^2,\alpha,\beta,0\end{matrix}\right). \quad (32)$$

Given that $P_{out}(\gamma_{th}) = F_{\gamma}(\gamma_{th})$, by substituting (11) and (16) into (31), P_{out} of Negative Exponential atmospheric turbulence is equal to:

$$P_{out,\gamma_{FSO/RF}}(\gamma_{th}) = \left(1-e^{-\frac{\gamma_{th}}{\overline{\gamma}_{RF}}}\right)^N + \left(1-e^{-\lambda\sqrt{\frac{\gamma_{th}}{\overline{\gamma}_{FSO}}}}\right) - \left(1-e^{-\frac{\gamma_{th}}{\overline{\gamma}_{RF}}}\right)^N \left(1-e^{-\lambda\sqrt{\frac{\gamma_{th}}{\overline{\gamma}_{FSO}}}}\right). \quad (33)$$

4.2. Bit error rate

By substituting (32) in (25), BER of DPSK modulation over Gamma–Gamma atmospheric turbulence considering pointing errors equals with:

$$P_e = \frac{1}{2}\int_0^{\infty} e^{-\gamma}\left\{\left(1-e^{-\frac{\gamma}{\overline{\gamma}_{RF}}}\right)^N + \frac{\xi^2}{\Gamma(\alpha)\Gamma(\beta)} G_{2,4}^{3,1}\left(\alpha\beta\kappa\sqrt{\frac{\gamma_{th}}{\overline{\gamma}_{FSO}}}\,\middle|\,\begin{matrix}1,\xi^2+1\\ \xi^2,\alpha,\beta,0\end{matrix}\right) - \frac{\xi^2}{\Gamma(\alpha)\Gamma(\beta)}\left(1-e^{-\frac{\gamma}{\overline{\gamma}_{RF}}}\right)^N G_{2,4}^{3,1}\left(\alpha\beta\kappa\sqrt{\frac{\gamma_{th}}{\overline{\gamma}_{FSO}}}\,\middle|\,\begin{matrix}1,\xi^2+1\\ \xi^2,\alpha,\beta,0\end{matrix}\right)\right\} d\gamma. \quad (34)$$

Substituting the binomial expansion of $\left(1-e^{-\gamma/\overline{\gamma}_{RF}}\right)^N$ as $\sum_{k=0}^{N}\binom{N}{k}(-1)^k e^{k\gamma/\overline{\gamma}_{RF}}$, and using [44, Eq. 07.34.21.0088.01] BER of DPSK modulation over Gamma–Gamma atmospheric turbulence with the effect of pointing errors equals with:

$$P_e = \frac{1}{2}\left\{\frac{\xi^2 2^{\alpha+\beta-3}}{\pi\Gamma(\alpha)\Gamma(\beta)} G_{5,8}^{6,3}\left(\frac{(\alpha\beta\kappa)^2}{16\overline{\gamma}_{FSO}}\,\middle|\,\begin{matrix}0,1,\frac{1}{2},\frac{1+\xi^2}{2},\frac{2+\xi^2}{2}\\ \frac{\xi^2}{2},\frac{1+\xi^2}{2},\frac{\alpha}{2},\frac{1+\alpha}{2},\frac{\beta}{2},\frac{1+\beta}{2},0,\frac{1}{2}\end{matrix}\right) + \sum_{k=0}^{N}\binom{N}{k}(-1)^k \frac{1}{1+\frac{k}{\overline{\gamma}_{RF}}} \times\left[1-\frac{\xi^2 2^{\alpha+\beta-3}}{\pi\Gamma(\alpha)\Gamma(\beta)} G_{5,8}^{6,3}\left(\frac{(\alpha\beta\kappa)^2}{16\overline{\gamma}_{FSO}}\,\middle|\,\begin{matrix}0,1,\frac{1}{2},\frac{1+\xi^2}{2},\frac{2+\xi^2}{2}\\ \frac{\xi^2}{2},\frac{1+\xi^2}{2},\frac{\alpha}{2},\frac{1+\alpha}{2},\frac{\beta}{2},\frac{1+\beta}{2},0,\frac{1}{2}\end{matrix}\right)\right]\right\}. \quad (35)$$

Substituting (33) into (25), BER of DPSK modulation over Negative Exponential atmospheric turbulence equals with:

$$P_e = \frac{1}{2}\int_0^{\infty} e^{-\gamma}\left\{\left(1-e^{-\frac{\gamma}{\overline{\gamma}_{RF}}}\right)^N + \left(1-e^{-\lambda\sqrt{\frac{\gamma}{\overline{\gamma}_{FSO}}}}\right) - \left(1-e^{-\frac{\gamma}{\overline{\gamma}_{RF}}}\right)^N\left(1-e^{-\lambda\sqrt{\frac{\gamma}{\overline{\gamma}_{FSO}}}}\right)\right\} d\gamma. \quad (36)$$

Substituting the binomial expansion of $\left(1-e^{-\gamma/\overline{\gamma}_{RF}}\right)^N$ and Meijer-G equivalent of $e^{-\lambda\sqrt{\gamma/\overline{\gamma}_{FSO}}}$ as $\frac{1}{\sqrt{\pi}} G_{0,2}^{2,0}\left(\lambda^2\gamma/4\overline{\gamma}_{FSO}\,\middle|\,\begin{matrix}-\\ 0,\frac{1}{2}\end{matrix}\right)$ and using [44, Eq. 07.34.03.1081.01] BER of DPSK modulation over negative exponential atmospheric turbulence equals with:

$$P_e = \frac{1}{2}\left\{1-\frac{1}{\sqrt{\pi}} G_{1,2}^{2,1}\left(\frac{\lambda^2}{4\overline{\gamma}_{FSO}}\,\middle|\,\begin{matrix}0\\ 0,\frac{1}{2}\end{matrix}\right) + \sum_{k=0}^{N}\binom{N}{k}(-1)^k \frac{1}{1+\frac{k}{\overline{\gamma}_{RF}}}\frac{1}{\sqrt{\pi}} G_{1,2}^{2,1}\left(\frac{\lambda^2}{4\overline{\gamma}_{FSO}\left(1+\frac{k}{\overline{\gamma}_{RF}}\right)}\,\middle|\,\begin{matrix}0\\ 0,\frac{1}{2}\end{matrix}\right)\right\}. \quad (37)$$

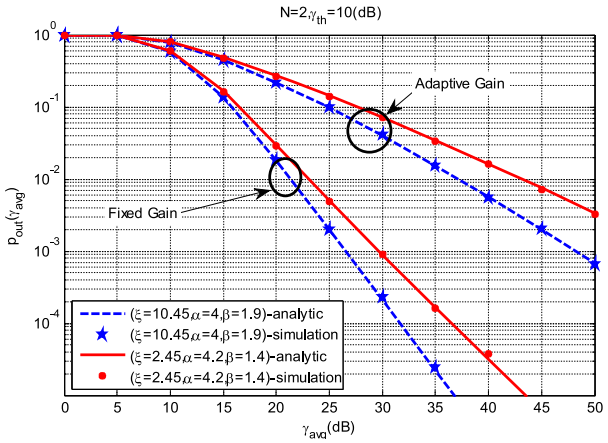

Fig. 2. Outage probability of proposed structure in terms of average SNR for moderate ($\alpha = 4, \beta = 1.9, \xi = 10.45$) and strong ($\alpha = 4.2, \beta = 1.4, \xi = 2.45$) regimes of Gamma–Gamma atmospheric turbulence with the effect of pointing error when $N = 2$ and $\gamma_{th} = 10$ dB, for fixed and adaptive gain schemes.

5. Numerical results

In this section analytic and MATLAB simulation results for performance investigation of proposed hybrid, FSO/RF system are compared. The RF link has Rayleigh fading and FSO link has Gamma–Gamma distribution with the effect of pointing errors (in moderate to strong regime) and Negative Exponential distribution (in saturate regime). Average SNR at FSO and RF receivers are considered to be equal ($\overline{\gamma}_{FSO} = \overline{\gamma}_{RF} = \gamma_{avg}$). The N is number of users, γ_{th} is outage threshold SNR, $\eta = 1$, and $C = 1$ (in fixed gain structure).

In Fig. 2 outage probability of proposed structure is plotted in terms of average SNR for moderate ($\alpha = 4, \beta = 1.9, \xi = 10.45$) and strong ($\alpha = 4.2, \beta = 1.4, \xi = 2.45$) regimes of Gamma–Gamma atmospheric turbulence with the effect of pointing error when $N = 2$ and $\gamma_{th} = 10$ dB, for fixed and adaptive gain schemes. As can be seen, in $\gamma_{avg} = 30$ dB, at different target P_{out}, difference of γ_{avg} between moderate and strong regimes in the adaptive gain scheme is less than 4 dB and in the fixed gain scheme is less than 3 dB. This difference increases by reducing P_{out}. Therefore, at low γ_{avg}, the proposed structure performs almost independent of atmospheric turbulence intensity. Hence, it is suitable for mobile communications, in which a small mobile battery should supply transmitter power (note that the received γ_{avg} in these systems is). As a result, it is not required to have adaptive processing in the proposed structure to maintain performance, and this reduces cost, complexity, and power consumption. The P_{out} of fixed gain relaying is less than adaptive gain relaying. Because fixed gain relaying (regardless of the channel conditions) selects high amplification gain to have the favorable performance at all channel conditions. But adaptive gain relaying, selects the amplification gain based on CSI (actually, it does not amplify the signal so much). Generally speaking, in moderate channels (favorable channel conditions), fixed gain relaying waste most of the consumed power.

In Fig. 3 outage probability of proposed structure is plotted in terms of average SNR for different number of users (N) in moderate ($\alpha = 4, \beta = 1.9, \xi = 10.45$) regime of Gamma–Gamma atmospheric turbulence with the effect of pointing error when $\gamma_{th} = 10$ dB for fixed and adaptive gain schemes. As can

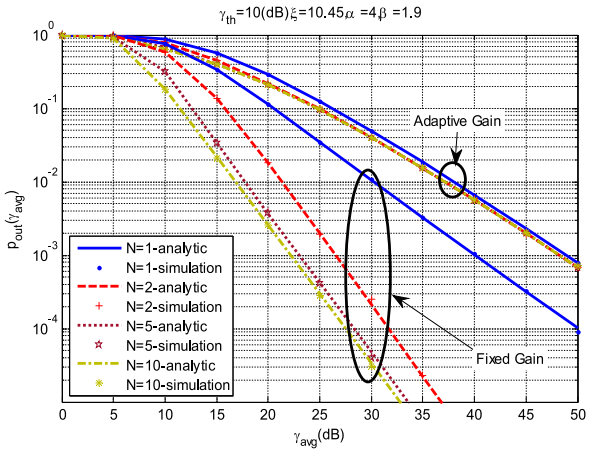

Fig. 3. Outage probability of proposed structure in terms of average SNR for different number of users (N) for moderate ($\alpha = 4, \beta = 1.9, \xi = 10.45$) regime of Gamma–Gamma atmospheric turbulence with the effect of pointing error when $\gamma_{th} = 10$ dB, for fixed and adaptive gain schemes.

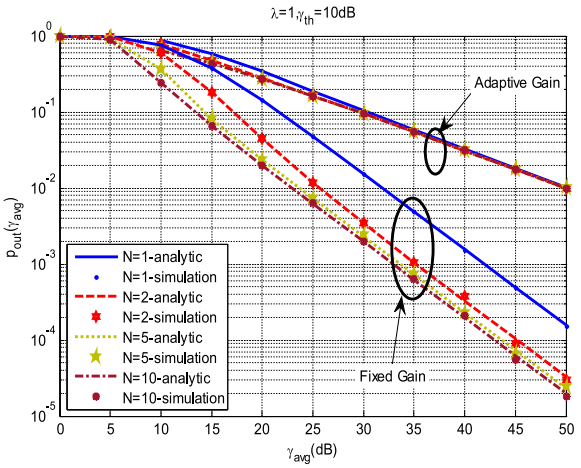

Fig. 5. Outage probability of proposed structure in terms of average SNR for the different number of users for Negative Exponential atmospheric turbulences with unit variance when $\gamma_{th} = 10$ dB, for fixed and adaptive gain schemes.

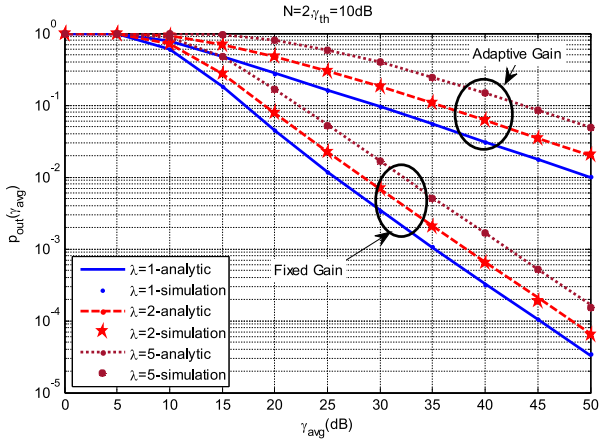

Fig. 4. Outage probability of the proposed structure is plotted in terms of average SNR for different variances ($1/\lambda^2$) of Negative Exponential atmospheric turbulence when $N = 2$ and $\gamma_{th} = 10$ dB for fixed and adaptive gain schemes.

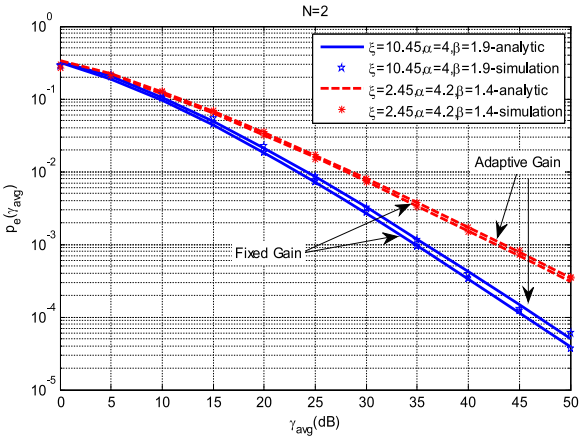

Fig. 6. Bit Error Rate of the proposed system in terms of average SNR for moderate ($\alpha = 4, \beta = 1.9, \xi = 10.45$) and strong ($\alpha = 4.2, \beta = 1.4, \xi = 2.45$) regimes of Gamma–Gamma atmospheric turbulence with the effect of pointing error when $N = 2$, for fixed and adaptive gain schemes.

be seen, the performance of the proposed system in the adaptive gain scheme is not so much sensitive to the number of users, but in fixed gain, the system is sensitive to the number of users. In dense population areas, many independent RF paths exist; hence, the probability of falling the received SNR below γ_{th} is much smaller than this probability for low population areas. By increasing γ_{avg}, the performance of adaptive gain relaying becomes almost independent of the number of users. This is an advantage for the proposed system because this structure could be used in areas where there is no direct RF link between user and base station (usually these areas are low populated). In fixed gain, system performance in dense population areas is much better, because its gain does not change according to channel conditions and at the different number of users a fixed gain is considered for relaying.

In Fig. 4 outage probability of the proposed structure is plotted in terms of average SNR for different variances ($1/\lambda^2$) of Negative Exponential atmospheric turbulence when $N = 2$ and $\gamma_{th} = 10$ dB for fixed and adaptive gain schemes. In this system, there are two users within the cell, as can be seen, at different target P_{out}, the difference of γ_{avg} between various variances of Negative Exponential atmospheric turbulence is the same. For example, when $P_{out} \leq 0.5$, the difference of γ_{avg} between cases of $\lambda = 1$ and $\lambda = 5$, in fixed gain is about 7 dB and in adaptive gain is about 13 dB. This affects the power consumption of the system because at any γ_{avg}, adding a constant fraction of consumed power maintains system performance at various variances.

In Fig. 5 outage probability of proposed structure is plotted in terms of average SNR for the different number of users (N) for Negative Exponential atmospheric turbulences with unit variance when $\gamma_{th} = 10$ dB for fixed and adaptive gain schemes. Performance of fixed gain relaying is sensitive to the number of users and dense population areas have better performance because users face independent atmospheric turbulences; therefore, it would be highly probable to find a user with favorable SNR.

In Fig. 6 Bit Error Rate of the proposed system is plotted in terms of average SNR for moderate ($\alpha = 4, \beta = 1.9, \xi = 10.45$) and strong ($\alpha = 4.2, \beta = 1.4, \xi = 2.45$) regimes of Gamma–Gamma atmospheric turbulence with the effect of pointing error when $N = 2$ for fixed and adaptive gain schemes. It can be seen when $\gamma_{avg} \leq 10$ dB, the link is virtually disrupted. Also, at low γ_{avg}, the performance of the proposed system in different atmospheric turbulence regimes does not differ so much, but by increasing γ_{avg} this difference increases. The behavior of the system in fixed gain and adaptive gain schemes, for both moderate

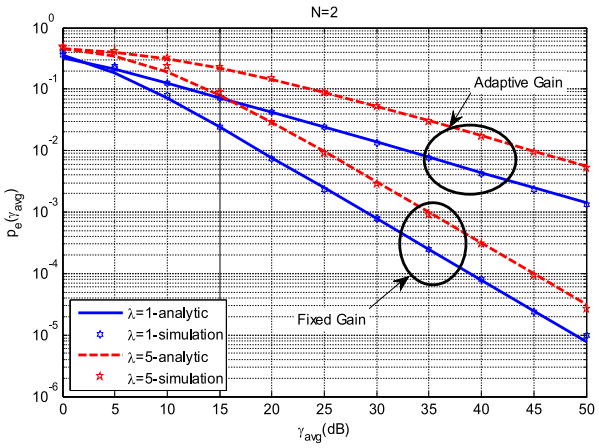

Fig. 7. Bit Error Rate of the proposed structure in terms of average SNR for different variances $(1/\lambda^2)$ of Negative Exponential atmospheric turbulences when $N = 2$ for fixed and adaptive gain schemes.

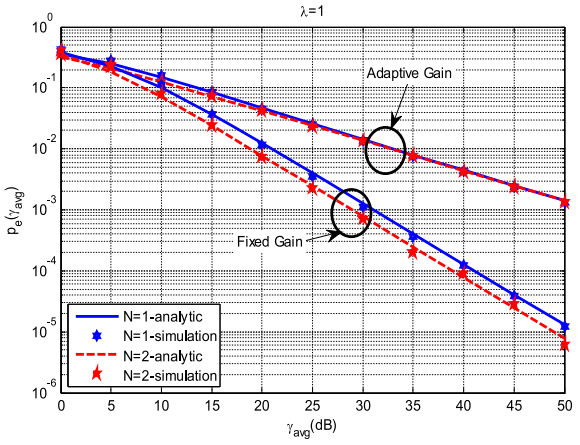

Fig. 8. Bit Error Rate of the proposed structure in terms of average SNR for different number of users (N) for Negative Exponential atmospheric turbulence with unit variance for fixed and adaptive gain schemes.

and strong atmospheric turbulence regimes, is almost the same when γ_{avg} is low, i.e. the system acts independent of atmospheric turbulence regime. At low γ_{avg}, the noise effect is so much high but at high γ_{avg}, its effect becomes negligible.

In Fig. 7 Bit Error Rate of the proposed structure in terms of average SNR for different variances $(1/\lambda^2)$ of Negative Exponential atmospheric turbulence when $N = 2$ for fixed and adaptive gain schemes. As can be seen, amplify and forward with fixed gain has better performance than adaptive gain. In the adaptive gain scheme, relay gain changes according to channel condition, but in fixed gain structure, relay gain is fixed and adjusted according to the worst case condition.

In Fig. 8 Bit Error Rate of the proposed structure is plotted in terms of average SNR for different number of users for Negative Exponential atmospheric turbulence with unit variance for fixed and adaptive gain schemes. It can be seen that in fixed gain structure, when $N = 1$, at $P_e = 0.1$, γ_{avg} increases about 2 dB. In the adaptive gain scheme at $\gamma_{avg} = 30$ dB, there is little difference in BER of the proposed system for different number of users, but since then the system performs independent of the number of users. Environments like seas mostly experience Negative Exponential atmospheric turbulence. Usually, there are few numbers of users in these places, therefore, a communication system is convenient for these areas that performs independent of number of users.

In Fig. 9, the outage probability of the proposed system at different atmospheric turbulence, for both cases of (a) fixed gain and (b) adaptive gain, when $\gamma_{th} = 10$ dB, and $N = 2$. In this plot fixed gain and adaptive gain are plotted separately (because they were close to each other, they should be plotted separately). From this figure (without considering legends), it could be guessed which plot is related to which turbulence, because Log-Normal, Gamma–Gamma, and Negative Exponential distributions could model weak, weak to strong, and saturate regimes, respectively. It can be seen that the proposed structure at all SNRs performs favorably at all atmospheric turbulence intensities.

Fig. 10 plots the outage probability of the proposed structure for adaptive gain relaying, considering actual value for received SNR (Eq. (7)), and its approximation (min $(\gamma_{FSO}, \gamma_{RF})$), for Gamma–Gamma ($\alpha = 4, \beta = 1.9$), and Negative Exponential ($\lambda = 1$) atmospheric turbulence. In this paper, both fixed gain and adaptive gain relaying schemes are studied over dual-hop FSO/RF

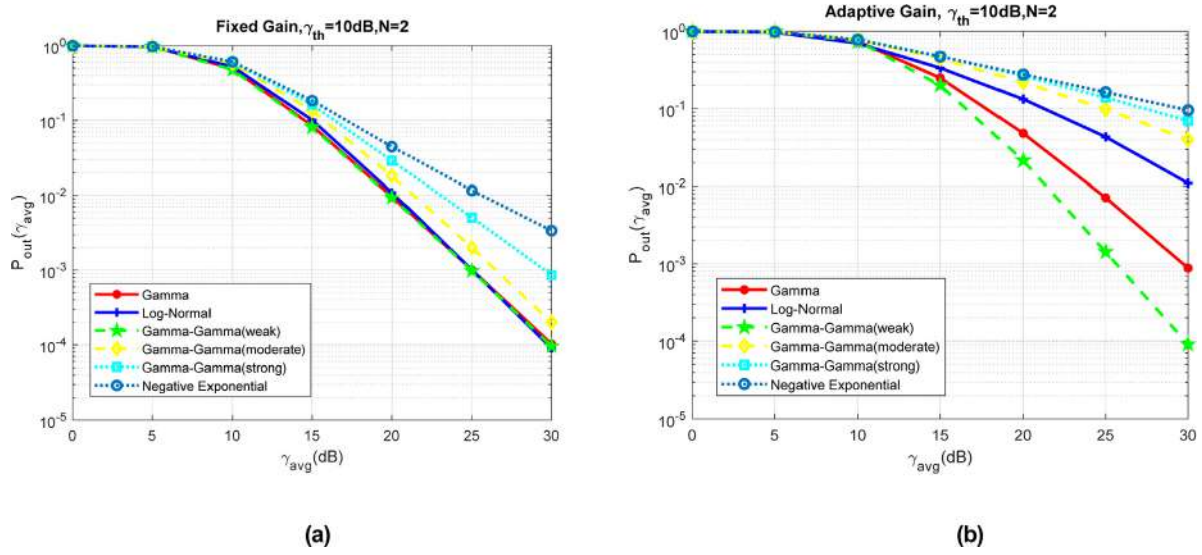

Fig. 9. Outage Probability of the proposed system at different atmospheric turbulence, for both cases of (a) fixed gain and (b) adaptive gain, when $\gamma_{th} = 10$ dB, and $N = 2$.

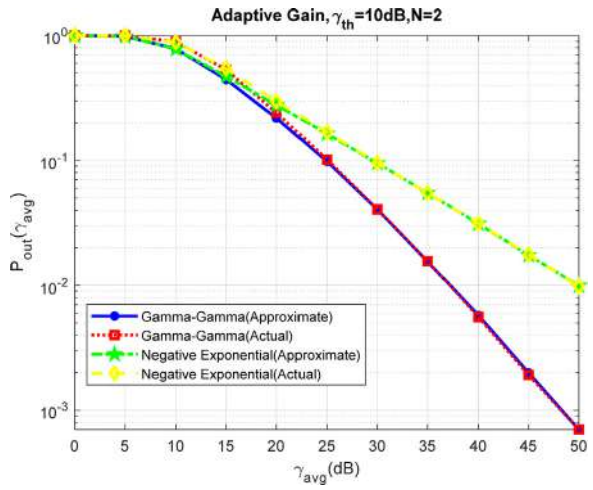

Fig. 10. Outage Probability of the proposed structure for adaptive gain relaying, considering actual value for received SNR (Eq. (7)), and its approximation ($\min(\gamma_{FSO}, \gamma_{RF})$), for Gamma–Gamma ($\alpha = 4, \beta = 1.9$), and Negative Exponential ($\lambda = 1$) atmospheric turbulence.

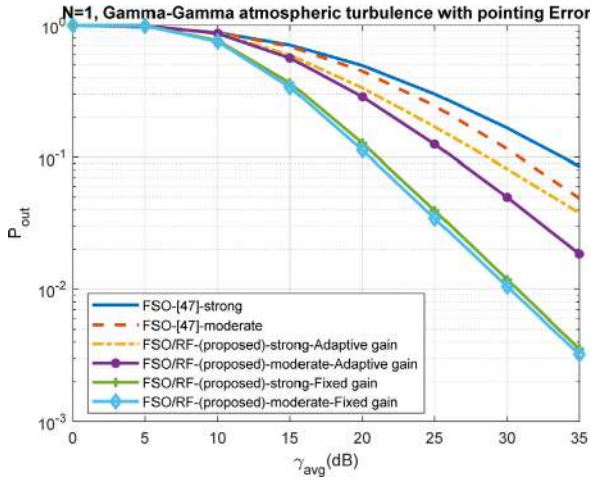

Fig. 11. Outage Probability of FSO system presented in [47], and the proposed adaptive gain/fixed gain structure of this paper, for moderate ($\alpha = 4, \beta = 1.9, \xi = 10.45$) and strong ($\alpha = 4.2, \beta = 1.4, \xi = 2.45$) regimes of Gamma–Gamma atmospheric turbulence with the effect of pointing error, when number of users is $N = 1$.

system. For the fixed gain case, exact closed-form results in terms of the Meijer-G function are derived. However, in the case of adaptive gain relaying, we have approximated the end-to-end SNR by the minimum of the instantaneous SNRs of the two hops as given by paragraph after Eq. (7), and the system performance metrics are derived based on the simplified expression which is $min(\gamma_{FSO}, \gamma_{RF})$ in this paper.

In simulations, the obtained results are illustrated based on $min(\gamma_{FSO}, \gamma_{RF})$ in the case of adaptive gain relaying which is logical since the aim of the Monte-Carlo simulations is to validate and check the accuracy of the derived analytical expressions.

Fig. 11 plots Outage Probability of FSO system presented in [47], and the proposed adaptive gain/fixed gain structure of this paper, for moderate ($\alpha = 4, \beta = 1.9, \xi = 10.45$) and strong ($\alpha = 4.2, \beta = 1.4, \xi = 2.45$) regimes of Gamma–Gamma atmospheric turbulence with the effect of pointing error, when number of users is $N = 1$. In [47], a single user FSO structure is investigated at Gamma–Gamma atmospheric turbulence with the effect of pointing error. It would be interesting to compare proposed hybrid FSO/RF structures of this paper with the FSO structure of [47]. In order to have a fair comparison, number of users is assumed to be $N = 1$ (because [47] is single user FSO), and the channel model is assumed to be Gamma–Gamma atmospheric turbulence with the effect of pointing error (because [47] assumed this channel model). Consider FSO structure of [47], add a relay (adaptive gain or fixed gain) in the middle of this link; this is the proposed structure of this paper. Fig. 11, shows the difference between these FSO and FSO/RF structures. In fact the proposed structure should have a better performance, because it is a hybrid FSO/RF structure and an amplification is made in it by the relay.

6. Conclusion

In this paper, a multi-user relay-assisted hybrid FSO/RF communication system is presented. In this system, a relay communicates with mobile users through a multi-user RF link and communicates with base station through an FSO link. This structure is especially recommended for areas that RF connection between the mobile user and the base station disrupts due to channel conditions. Closed form expressions are derived for BER and P_{out} of the proposed system for both fixed and adaptive gain schemes and MATLAB simulation results, verified accuracy of these expressions. It is shown that fixed gain, despite low complexity but because of more power consumption, has better performance. Adaptive gain relaying has low sensitivity to the number of users, but fixed gain is more sensitive. Overall, it can be concluded that in places with saturate atmospheric turbulence, because of the importance of power and the number of users, the adaptive gain structure is suggested and in moderate to strong atmospheric turbulence, depending on power or system performance requirement, fixed or adaptive gain would be deployed.

CRediT authorship contribution statement

Mohammad Ali Amirabadi: Conceptualization, Data curation, Formal analysis, Funding acquisition, Investigation, Methodology, Project administration, Resources, Software, Supervision, Validation, Visualization, Writing - original draft, Writing - review & editing. **Vahid Tabataba Vakili:** Writing review & editing.

Conflict of interest

None.

Declaration of competing interest

The authors declared that they had no conflicts of interest with respect to their authorship or the publication of this article.

References

[1] R.K. Sharma, H. Kaushal, P.K. Sharma, Analysis of indoor FSO link under diffused channel topology, in: International Conference on Computing, Communication & Automation, IEEE, 2015, May, pp. 128–1272.
[2] N.J. Navita, P.K. Sharma, S. Ahuja, Error performance of SIM-MPSK over S-distributed FSO links.
[3] M.A. Amirabadi, Performance analysis of a novel hybrid FSO/RF communication system, 2018, arXiv preprint arXiv:1802.07160.
[4] R. Nebuloni, Empirical relationships between extinction coefficient and visibility in fog, Appl. Opt. 44 (18) (2005) 3795–3804.
[5] M.A. Amirabadi, V.T. Vakili, A new optimization problem in FSO communication system, IEEE Commun. Lett. 22 (7) (2018) 1442–1445.
[6] M.A. Amirabadi, An optimization problem on the performance of FSO communication system, 2019, arXiv preprint arXiv:1902.10043.

[7] P.K. Sharma, A. Bansal, P. Garg, T. Tsiftsis, R. Barrios, Relayed FSO communication with aperture averaging receivers and misalignment errors, IET Commun. 11 (1) (2017) 45–52.
[8] P.K. Sharma, Average symbol error rate for M-ary quadrature amplitude modulation in generalized atmospheric turbulence and misalignment errors, Opt. Eng. 55 (11) (2016) 111615.
[9] P.K. Sharma, A. Bansal, P. Garg, T.A. Tsiftsis, R. Barrios, Performance of FSO links under exponentiated Weibull turbulence fading with misalignment errors, in: 2015 IEEE International Conference on Communications, ICC, IEEE, 2015, June, pp. 5110–5114.
[10] P.K. Sharma, A. Bansal, M.R. Bhatnagar, Arbitrary beamforming based FSO MIMO system in atmospheric turbulence and misalignment errors, in: 2016 Twenty Second National Conference on Communication, NCC, IEEE, 2016, March, pp. 1–5.
[11] S. Anees, M.R. Bhatnagar, Performance of an amplify-and-forward dual-hop asymmetric RF–FSO communication system, J. Opt. Commun. Netw. 7 (2) (2015) 124–135.
[12] P. Puri, P. Garg, M. Aggarwal, P.K. Sharma, Outage analysis of two-way relay assisted FSO systems over weak turbulence region, in: 2013 Annual IEEE India Conference, INDICON, IEEE, 2013, December, pp. 1–5.
[13] A. Bansal, P.K. Sharma, M.R. Bhatnagar, Optimal and suboptimal decoding for SIM-BPSK over gamma-gamma FSO links with an erroneous relay, in: 2015 Twenty First National Conference on Communications, NCC, IEEE, 2015, February, pp. 1–6.
[14] A. Bansal, P.K. Sharma, M.R. Bhatnagar, DF cooperation over Gamma-Gamma fading FSO links with an erroneous relay, in: 2015 IEEE International Conference on Communications, ICC, IEEE, 2015, June, pp. 5104–5109.
[15] M.A. Amirabadi, V.T. Vakili, Performance evaluation of a novel relay assisted hybrid FSO/RF communication system with receive diversity, 2018, arXiv preprint arXiv:1806.02597.
[16] M.A. Amirabadi, V.T. Vakili, New expressions on the performance of a novel multi-hop relay-assisted hybrid FSO/RF communication system with receive diversity, 2018, arXiv preprint arXiv:1806.08223.
[17] M.A. Amirabadi, Performance comparison of two novel relay-assisted hybrid FSO/RF communication systems, 2018, arXiv preprint arXiv:1802.07335.
[18] V.V. Mai, A.T. Pham, Adaptive multi-rate designs and analysis for hybrid FSO/RF systems over fading channels, IEICE Trans. Commun. (2015).
[19] M.A. Amirabadi, V.T. Vakili, A novel hybrid FSO/RF communication system with receive diversity, Optik (2019).
[20] W. Gappmair, H.E. Nistazakis, Subcarrier PSK performance in terrestrial FSO links impaired by gamma-gamma fading, pointing errors, and phase noise, J. Lightwave Technol. 35 (9) (2017) 1624–1632.
[21] I.S. Ansari, M.S. Alouini, F. Yilmaz, On the performance of hybrid RF and RF/FSO fixed gain dual-hop transmission systems, in: 2013 Saudi International Electronics, Communications and Photonics Conference, IEEE, 2013, April, pp. 1–6.
[22] E. Soleimani-Nasab, M. Uysal, Generalized performance analysis of mixed RF/FSO cooperative systems, IEEE Trans. Wirel. Commun. 15 (1) (2016) 714–727.
[23] K. Kumar, D.K. Borah, Quantize and encode relaying through FSO and hybrid FSO/RF links, IEEE Trans. Veh. Technol. 64 (6) (2015) 2361–2374.
[24] R. Boluda-Ruiz, A. García-Zambrana, B. Castillo-Vázquez, C. Castillo-Vázquez, MISO relay-assisted FSO systems over gamma–gamma fading channels with pointing errors, IEEE Photonics Technol. Lett. 28 (3) (2016) 229–232.
[25] R. Boluda-Ruiz, A. García-Zambrana, B. Castillo-Vázquez, C. Castillo-Vázquez, Ergodic capacity analysis of decode-and-forward relay-assisted FSO systems over alpha–Mu fading channels considering pointing errors, IEEE Photonics J. 8 (1) (2016) 1–11.
[26] V. Jamali, D.S. Michalopoulos, M. Uysal, R. Schober, Mixed RF and hybrid RF/FSO relaying, in: 2015 IEEE Globecom Workshops, GC Wkshps, IEEE., 2015, December, pp. 1–6.
[27] G. Djordjevic, M. Petkovic, A. Cvetkovic, G. Karagiannidis, Mixed RF/FSO relaying with outdated channel state information, IEEE J. Sel. Areas Commun. (2015).
[28] N.I. Miridakis, M. Matthaiou, G.K. Karagiannidis, Multiuser relaying over mixed RF/FSO links, IEEE Trans. Commun. 62 (5) (2014) 1634–1645.
[29] E. Zedini, H. Soury, M.S. Alouini, On the performance analysis of dual-hop mixed FSO/RF systems, IEEE Trans. Wirel. Commun. 15 (5) (2016) 3679–3689.
[30] E. Zedini, H. Soury, M.S. Alouini, On the performance of dual-hop FSO/RF systems, in: 2015 International Symposium on Wireless Communication Systems, ISWCS, IEEE, 2015, August, pp. 31–35.
[31] E. Lee, J. Park, D. Han, G. Yoon, Performance analysis of the asymmetric dual-hop relay transmission with mixed RF/FSO links, IEEE Photonics Technol. Lett. 23 (21) (2011) 1642–1644.
[32] L. Kong, W. Xu, L. Hanzo, H. Zhang, C. Zhao, Performance of a free-space-optical relay-assisted hybrid RF/FSO system in generalized $ M $-distributed channels, IEEE Photonics J. 7 (5) (2015) 1–19.
[33] H. Samimi, M. Uysal, End-to-end performance of mixed RF/FSO transmission systems, J. Opt. Commun. Netw. 5 (11) (2013) 1139–1144.
[34] E. Zedini, I.S. Ansari, M.S. Alouini, Performance analysis of mixed Nakagami-$ M $ and Gamma–Gamma dual-hop FSO transmission systems, IEEE Photonics J. 7 (1) (2015) 1–20.
[35] Z. Jing, Z. Shang-hong, Z. Wei-hu, C. Ke-fan, Performance analysis for mixed FSO/RF Nakagami-m and exponentiated Weibull dual-hop airborne systems, Opt. Commun. 392 (2017) 294–299.
[36] J. Zhang, L. Dai, Y. Zhang, Z. Wang, Unified performance analysis of mixed radio frequency/free-space optical dual-hop transmission systems, J. Lightwave Technol. 33 (11) (2015) 2286–2293.
[37] B. Bag, A. Das, A. Chandra, C. Bose, CaPacity analysis for Rayleigh/gamma-gamma mixed RF/FSO link with fixed-gain AF relay, IEICE Trans. Commun. 100 (10) (2017) 1747–1757.
[38] E. Zedini, H. Soury, M.S. Alouini, Dual-hop FSO transmission systems over gamma–gamma turbulence with pointing errors, IEEE Trans. Wirel. Commun. 16 (2) (2017) 784–796.
[39] N. Varshney, P. Puri, Performance analysis of decode-and-forward-based mixed MIMO-RF/FSO cooperative systems with source mobility and imperfect CSI, J. Lightwave Technol. 35 (11) (2017) 2070–2077.
[40] M.A. Amirabadi, V.T. Vakili, Performance analysis of hybrid FSO/RF communication systems with alamouti coding or antenna selection, 2018, arXiv preprint arXiv:1802.07286v1.
[41] P.K. Sharma, A. Bansal, P. Garg, Relay assisted bi-directional communication in generalized turbulence fading, J. Lightwave Technol. 33 (1) (2015) 133–139.
[42] P.K. Sharma, P. Garg, Bi-Directional Decode-XOR-Forward Relaying Over ($\mathcal{M}$)-Distributed Free Space Optical Links, IEEE Photonics Technol. Lett. 26 (19) (2014) 1916–1919.
[43] I.S. Gradshteyn, I.M. Ryzhik, Table of Integrals, Series, and Products. Seventh Edition, Elsevier Inc., 2007.
[44] http://functions.wolfram.com/HypergeometricFunctions/.
[45] N. Joshi, P.K. Sharma, Performance of Wireless Optical Communication in $\mathcal{S}$-Distributed Turbulence, IEEE Photonics Technol. Lett. 28 (2) (2016) 151–154.
[46] A. Papoulis, S.U. Pillai, Probability, Random Variables, and Stochastic Processes, Tata McGraw-Hill Education, 2002.
[47] A.A. Farid, S. Hranilovic, Outage capacity optimization for free-space optical links with pointing errors, J. Lightwave Technol. 25 (7) (2007) 1702–1710.

Mohammad Ali Amirabadi was born in Zahedan, Iran, in 1993. He received the B.Sc. degree in Optics & Laser Engineering from Malek-e-Ashtar University of Technology, Isfahan, Iran, in 2015. Now he is studying M.Sc. in Communication Engineering in Iran University of Science and Technology, Tehran, Iran. He worked with Shaheed Chamran Research Center Institute, Isfahan, as a Research Engineer, from 2011 to 2015. His research interests include Free Space Optical Communications, Relay Assisted Networks, and Hybrid FSO/RF systems.

Vahid Tabataba Vakili received the B.S. degree from Sharif University of Technology, Tehran, Iran, in 1970, the M.S. degree from the University of Manchester, Manchester, UK, in 1973, and the Ph.D. degree from the University of Bradford, Bradford, UK, in 1977, all in Electrical Engineering. In 1985, he joined the Department of Electrical Engineering, Iran University of Science and Technology, Tehran. He was promoted to Professor in 2010. He has served as the Head of the Communications Engineering Department and as the Head of postgraduate studies. His research interests are in the areas of mobile cellular systems, interference cancellation for CDMA systems, ultra wideband communication system and space–time processing and coding.